RESEARCH ARTICLE

Mechanical and Thermal Properties of Gd-Doped ZnO Nanorods

Navin Chaurasiya[1,2], Sachin Rai[1], Pramod K. Yadawa[1,]*

All the elastic, mechanical and thermal properties of Gd-doped ZnO nanorods (NRs) have studied using interaction potential model. Gd-doped ZnO nanorods are hexagonal wurtzite structure. The characteristic features of elastic characteristics of Gd-doped ZnO NRs imply that this is mechanically stable. For mechanical characterization, bulk modulus (B), shear modulus (G), Young's modulus (Y), Pugh's ratio (B / G), Poisson's ratio and anisotropic index are evaluated using second order elastic constants. For the investigation of anisotropic behaviour and thermophysical properties, ultrasonic velocities and thermal relaxation time have been also calculated along with different orientations from the unique axis of the crystal. The mechanical properties of the Gd-doped ZnO nanorods are better than at 6% Gd amount due to minimum attenuation. The obtained results are analyzed to explore the characteristic of ZnO nanorods. Computed elastic, ultrasonic and thermal properties are correlated to evaluate the microstructural behaviour of the materials useful for industrial applications.

Introduction

Transition metal oxides (TMOs) based nanomaterials exhibit several remarkable electric, optical, optoelectronic, spintronic, electrical, luminescent and magnetic properties making them potential applicants for modern industries [**1,2**]. TMO nanostructured materials have both novel nano-effect and outstanding semiconducting characteristics, making them promising candidates for nanoscience technology [**3**]. Among various TMOs, ZnO, a wide bandgap n-type semiconductor with super excitation energy, has received the most attention due to their superior physical and chemical properties and numerous used in solar cell submissions, thin film transistors (TFTs), sensors, photocatalysts, water piercing (hydrogen generation) and biomedical applications [**4,5**]. Pure and doped ZnO is the most preferable materials for industrial application because of its nontoxic nature, easy synthesis process, chemical stability, and its suitability for doping with various metals [**6,7**]. To advance some properties of Zinc oxide, it is generally diluted or doped with some ions like Mn, Al and Ni [**7**]. Zinc oxide doped with 4f rare earth elements exhibits more advanced optical, structural and magnetic properties compared to that of doped with most commonly used 3d transition metals. Particularly, ZnO doped with Gd^{3+} have shown greater magnetic properties and analysed in some theoretical and experimental studies [**8,9**].

Based on the dimension, nanomaterials can be classified into three categories: zero- dimensional (0-D), one-dimensional (1-D), and two-dimensional (2-D) [**10**]. In 1-D nanostructure, two dimensions are of the order of nanometre and other one is much larger which leads to a needle shaped structure like nanorods, nanofibers and nanowires. Among different 1-D materials, nanorods are more advantageous compared to nanowires and nanotubes because they can be fabricated using metals as well as nonmetals and their synthesis process is more economic and flexible [**11,12**]. NRs also possess decent mechanical properties like shape anisotropy which make them attractive and applicable for many applications [**13**]. Different types of metal oxide based nanorod systems have been analysed by the researcher K. Navaneethan *et al.* have reported photocatalytic activity of TiO_2 nanorods against methyl orange with 51% degradation within 150 min [**14**]. A. Nikitin *et al.* synthesized iron oxide nanorods via microwave irradiation method and found it most suitable for enhanced magnetic hyperthermia [**15**]. Functional properties of tungsten oxide based nanorod were studied by A. Azeem *et al.* in which they reported voltage dependent tunable transmittance modulation properties of the same [**16**]. N. W. Kim *et al*. presented a facile synthesis process for the fabrication of high-quality cerium oxide nanorods with different diameters via common ion effect method [**17**]. A. Bramantyo *et al.* have fabricated zinc oxide nanorods using the method of seed layer deposition under a controlled size mechanism and obtained the nanorods having size of 10 nm, crucial for perovskite solar cells [**18**]. Thus, number of optical, electronic, magnetic and biomedical properties of the metal oxide based nanorod

[1]Department of Physics, Prof. Rajendra Singh (Rajju Bhaiya) Institute of Physical Sciences for Study and Research, Veer Bahadur Singh Purvanchal University, Jaunpur 222003, India
[2]Department of Mechanical Engineering, UNSIET, V. B. S. Purvanchal University, Jaunpur 222003, India

*Corresponding author:
E-mail: pkyadawa@gmail.com; Tel.: (+91) 8700141797

DOI: 10.5185/amlett.2021.111681

have been reported by the researchers but, to the best of our knowledge, very few studies have been done on ultrasonic, mechanical and thermal properties of metal oxide based nanorods, especially the work representing doping effects on these properties have not been reported yet. This motivates us to study the ultrasonic, elastic and thermal properties of the Gd doped ZnO nanorods.

Ultrasonic is a non-destructive technique for material characterization and is one of the best methods for material characterization not only after the production but during the process as well. Ultrasonic properties are significant for the study of physical characteristics of the materials such as thermal relaxation time, energy density and thermal conductivity. Some mechanical constants like bulk modulus, shear modulus, Young's modulus, Pugh's ratio, Poisson's ratio and anisotropic index can be easily determined using linear elastic constants which in turn help us in predicting the response of the crystal under applied stress [**19**]. Ultrasonic attenuation (UA) is the exact main physical parameter to describe a material, whichever appreciates the specific relationship between the anisotropic behaviour of proximal hematinic planes and the affinity and structural motion, some physical measures like thermal energy density, specific heat and thermal conductivity, is well associated with higher-order elastic constants [**20**].

In this work, we were worked diligently to make the relationship between thermo physical and microstructural properties for Gd-doped ZnO nanorods will help in understanding the mechanical behaviour of nanostructured Gd-doped ZnO nanorods and its performance and significant role in the diagram of manufacturing apparatus with useful physical properties under moderate working conditions. For that, we have considered ultrasonic velocities, attenuation coefficients, acoustic coupling constants, elastic stiffness constant and thermal relaxation time for Gd-doped ZnO nanorods. The bulk modulus (B), shear modulus (G), Young's modulus (Y), Pugh's ratio (B / G), Poisson's ratio and anisotropic index were also calculated and discussed for %Gd-doped ZnO nanorods.

Theory

There are numerous methods to analyses second order elastic constants (SOECs) of hexagonal materials. Meanwhile, a first-principal technique based on DFT in the quasi-harmonic approximation (QHA) and generalized gradient approximation (GGA) are commonly used for determination of second and third order elastic constants. The technique based on interaction potential model is one of the well-established methods for the deduction of second order elastic constants (SOECs) of hexagonal structured material. In present work, the Lenard Jones interaction potential model approach was used for the evaluation of SOECs. The higher order elastic constants can be calculated by the estimation of elastic energy density with strain. A generalized n^{th} order elastic constant is expressed as partial derivatives of the free energy density of the medium under finite deformation, given by the following expression [**21,22**]

$$C_{ijklmn\ldots} = \frac{\partial^n F}{\partial\eta_{ij}\partial\eta_{kl}\partial\eta_{mn\ldots}} \quad (1)$$

where, F and η_{ij} are free energy density and Lagrangian strain tensor, respectively. Using Taylor series, F can be described in terms of strain η as follows:

$$F = \sum_{n=0}^{\infty} F_n = \sum_{n=0}^{\infty} \frac{1}{n!}\left(\frac{\partial^n F}{\partial\eta_{ij}\partial\eta_{kl}\partial\eta_{mn\ldots}}\right)\eta_{ij}\eta_{kl}\eta_{mn}\ldots \quad (2)$$

Thus, the free energy density upto cubic term is written as:

$$F_2 + F_3 = \frac{1}{2!}C_{ijkl}\eta_{ij}\eta_{kl} + \frac{1}{3!}C_{ijklmn}\eta_{ij}\eta_{kl}\eta_{\mathrm{mn}} \quad (3)$$

For HCP material the basis vectors are$a_1 = a\left(\frac{\sqrt{3}}{2}, \frac{1}{2}, 0\right)$, $a_2 = a(0,1,0)$ and $a_3 = a(0,0,c)$in Cartesian system axes. Here a and c are the unit cell parameters. The unit cell of HCP material consists of two non-equivalent atoms: six atoms in basal plane and three-three atoms above and below the basal plane. Thus, both first and second neighbourhood consists of six atoms. The $r_1 = a(0,0,0)$and $r_2 = \left(\frac{a}{2\sqrt{3}}, \frac{a}{2}, \frac{c}{2}\right)$ are the position vectors of these two types of atoms.

The potential energy per unit cell up to second nearest neighbour is written as follows:

$$U_2 + U_3 = \Sigma_{I=1}^{6} \quad U(r_I) + \Sigma_{J=1}^{6} \quad U(r_J) \quad (4)$$

where, I refer to atoms in the basal plane and J refers to atoms above and below the basal plane. When the crystal is deformed homogeneously then interatomic vectors in undeformed state (r) and deformed state (r') are related as:

$$(r')^2 - (r)^2 = 2\varepsilon_i\varepsilon_j\eta_{ij} = 2\Theta \quad (5)$$

where, ε_i and $\varepsilon_j$are the Cartesian component of vector r. The energy density U can be explained in terms of Θ as [**21, 22**]

$$U_n = (2V_c)^{-1}\Sigma\frac{1}{n!}\Theta^n D^n\varphi(r) \quad (6)$$

Using equations (4) and (6), the energy density U involving cubic terms can be written as:

$$U_2 + U_3 = (2V_c)^{-1}\left[\sum_{I=1}^{6}\frac{1}{2!}{\Theta_I}^2 D^2\varphi(r_I) + \sum_{J=1}^{6}\frac{1}{2!}{\Theta_J}^2 D^2\varphi(r_J)\right]$$
$$+(2V_c)^{-1}\left[\Sigma_{I=1}^{6}\frac{1}{3!}{\Theta_I}^3 D^3\varphi(r_I) + \Sigma_{J=1}^{6}\frac{1}{3!}{\Theta_J}^3 D^3\varphi(r_J)\right] \quad (7)$$

The energy density is considered to be function of Lennard Jones potential and given as:

$$\varphi(r) = -\frac{a_0}{r^m} + \frac{b_0}{r^n} \quad (8)$$

where, a_0, b_0 represent constants; m, n are integers and r are the distance between atoms. Taking the approximation of the interaction potential up to second nearest neighbours, the crystal symmetry exhibits the six second order elastic constants (SOECs) of the hexagonal material and formulations of elastic constants were taken by our previous papers [**21,22**].

Bulk modulus and shear modulus were calculated using Voigt and Reuss' methodologies [**23,24**]. The

calculations of unvarying stress and unvarying strain were used in the Voigt and Reuss' methodologies. Furthermore, From Hill's methods, average values of the both methodologies were used toward compute ensuing values of B and G [**25**]. Young's modulus and Poisson's ratio are considered using values of bulk modulus and shear modulus respectively [**26,27**]. The following expressions (Equations (1)) were used for the evaluation of Y, B, G and σ.

$$\left.\begin{aligned} &M = C_{11} + C_{12} + 2C_{33} - 4C_{13}; \\ &\qquad C^2 = (C_{11} + C_{12})C_{33} - 4C_{13} + C^2{}_{13}; \\ &B_R = \frac{C^2}{M}; \mathrm{B}_V = \frac{2(C_{11} + C_{12}) + 4C_{13} + C_{33}}{9}; \\ &G_V = \frac{M + 12(C_{44} + C_{66})}{30}; \mathrm{G}_R = \frac{5C^2 C_{44} C_{66}}{2[3B_V C_{44} C_{66} + C^2(C_{44} + C_{66})]}; \\ &Y = \frac{9GB}{G + 3B}; \quad \mathrm{B} = \frac{B_V + B_R}{2}; \quad \mathrm{G} = \frac{G_V + G_R}{2}; \sigma = \frac{\mathrm{3B\text{-}2G}}{2(3\mathrm{B} + G)} \end{aligned}\right\} \quad (9)$$

The mechanical and anisotropic properties of materials are studied by estimating the ultrasonic velocity. There are three types of modes of propagation of the ultrasonic wave in the hexagonal structured materials. One of them is a longitudinal mode (V_L) and other two are shear modes (V_{S1}, V_{S2}). The velocities of ultrasonic wave as a function of angle (θ) (between direction of propagation and unique axis (z axis)) are given by the following set of equation:

$$\left.\begin{aligned} V_L^2 &= \{C_{33}\cos^2\theta + C_{11}\sin^2\theta + C_{44} + \\ &\{[C_{11}\sin^2\theta - C_{33}\cos^2\theta + C_{44}(\cos^2\theta - \sin^2\theta)]^2 \\ &+4\cos^2\theta\sin^2\theta\,(C_{13} + C_{44})^2\}^{1/2}\}/2\rho \\ V_{S1}^2 &= \{C_{33}\cos^2\theta + C_{11}\sin^2\theta + C_{44} - \\ &\{[C_{11}\sin^2\theta - C_{33}\cos^2\theta + C_{44}(\cos^2\theta - \sin^2\theta)]^2 \\ &+4\cos^2\theta\sin^2\theta\,(C_{13} + C_{44})^2\}^{1/2}\}/2\rho \\ V_{S2}^2 &= \{C_{44}\cos^2\theta + C_{66}\sin^2\theta\}/\rho \end{aligned}\right\} \quad (10)$$

where, V_L, V_{S1}, and V_{S2} are the longitudinal, quasi-shear, and shear wave velocities; ρ and θ are the density of the material. For hexagonal material the Debye average velocity given by the equation as [**28-30**]

$$V_D = \left[\frac{1}{3}\left(\frac{1}{V_L^3} + \frac{1}{V_{S1}^3} + \frac{1}{V_{S2}^3}\right)\right]^{-1/3} \quad (11)$$

The thermal relaxation time, denoted by τ, and is given by following expression:

$$\tau = \tau_S = \tau_L/2 = \frac{3k}{C_V V_D^2} \quad (12)$$

where the τ_L and τ_S represent the relaxation time for the longitudinal wave and shear wave are represented and k is the thermal conductivity of the material.

Results and discussion

Higher order elastic constants

In current analysis, we have calculated the six second order elastic constants using Lennard-Jones potential model. The lattice parameters 'a' (basal plane parameter) and 'p' (axial ratio) for (0%, 1%, 2%, 3%, 4%, 5% and 6%) Gd-doped ZnO nanorods are 3.2483Å, 3.2480Å, 3.2477Å, 3.2475Å, 3.2475Å, 3.2475Å, 3.2475Å and 1.6034, 1.60325, 1.60313, 1.603, 1.60315, 1.60325, 1.6034 respectively. [**31**] The values of positive integers m and n are considered 6 and 7, respectively, for all the samples. The values of b_0 are 2.095×10^{-62} erg cm^7 for all samples of Gd-doped ZnO nanorods. Values of second order elastic constants were calculated for these Gd-doped ZnO nanorods is offered now **Table 1**.

Table 1. SOECs (in GPa) of Gd-doped ZnO at room temperature.

Gd% doped ZnO	C_{11}	C_{12}	C_{13}	C_{33}	C_{44}	C_{66}
0%Gd-ZnO	211.4	50.3	42.3	209.2	46.3	76.3
1%Gd-ZnO	215.3	52.0	43.0	211.1	49.3	78.2
2%Gd-ZnO	217.2	54.1	44.2	214.0	52.0	83.7
3%Gd-ZnO	221.3	55.7	45.4	216.4	55.3	87.7
4%Gd-ZnO	214.0	54.3	45.4	215.3	53.5	85.5
5%Gd-ZnO	218.2	53.8	44.8	214.1	52.2	83.2
6%Gd-ZnO	217.4	53.0	43.2	213.0	51.3	82.1
ZnO [32]	206±4	--	108±10	211±4	44.3±1	44.6±1
ZnO [33]	207	--	101	209	46.1	44.5

Gd-doped ZnO nanorods had the highest elastic constant values, which are important for the material, as these are associated with the stiffness parameter. SOECs are used to determine the associated parameters. Highest elastic constant values found for nanostructured Gd-doped ZnO nanorods are indicative of their better mechanical properties.

Evidently, for steady of the nanostructured compound, the five independent SOECs (Cij, namely C_{11}, C_{12}, C_{13}, C_{33}, C_{44}) would satisfy the well-known Born- Huang's stability norms [**26,27**] i.e., $C_{11} - |C_{12}| > 0$, $(C_{11}+C_{12})\,C_{33} - 2C^2{}_{13} > 0$, $C_{11} > 0$ and $C_{44} > 0$. Which is understandable since Table-1. It is evident that the values of elastic constant are positive too satisfies Born-Huang's mechanical stability constraints and therefore totally these compounds are mechanically stable. It is obvious from **Table 1** that, there is good agreement between the present and reported theoretical/experimental SOECs of pure (without doped) ZnO nanorods [**32,33**]. Thus, there is respectable agreement between presented and the reported values which is correlated with elastic constants. Therefore, our theoretical methodology is well justified for the evaluation of SOECs of nanostructured compounds. Therefore, the applied theory for valuation of SOECs is justified.

The values of B, G, Y, B/G and σ for nanostructured Gd-doped ZnO nanorods at room temperature is calculated using Equation (9) and existing in **Table 2**.

Table 2. Voigt–Reus' constants (M and C^2), B (x 10^{10}Nm^{-2}), G (x 10^{10}Nm^{-2}), Y (x 10^{10}Nm^{-2}), σ, B/G for % Gd-doped ZnO nanorods.

	M	C^2 (10^4)	B_r	B_v	G_r	G_v	Y	B/G	G/B	σ
0%Gd-ZnO	511	5.64	110	100	125	66	220	1.13	0.91	0.15
3%Gd-ZnO	52	6.19	118	106	70	75	173	1.22	0.82	0.18
6%Gd-ZnO	524	5.93	113	103	68	71	171	1.56	0.64	0.24

It is established that the values of B, Y, and G of nanostructured Gd-doped ZnO nanorods, the Gd-doped ZnO NWs have little Stiffness. 'B/G' and 'σ' are the measure of brittleness and ductility of solid. If the value of σ = ≤0.26 and B/G = ≤1.75, the materials is generally brittle, otherwise it is ductile in nature [**34,35**]. Our finding of lower values of B/G and σ compared to their critical values indicates that nanostructured Gd-doped ZnO nanorods are brittle in nature. The values of 'σ' evaluated for Gd-doped ZnO nanorods are smaller than its critical value. It indicates that Gd-doped ZnO nanorods is stable against shear. The stronger degree of covalent bonding leads to higher hardness. The compressibility, hardness, ductility, toughness, brittleness and bonding characteristic of the material are too well connected with the second order elastic constants.

Ultrasonic velocity and allied constraints

In present analysis, we have correlated the mechanical and isotropic behavior of the compound with the ultrasonic velocity. We have calculated the longitudinal ultrasonic wave velocity (V_L), shear ultrasonic wave velocity (V_S), the Debye average velocity (V_D) and the thermal relaxation time (τ) for Gd-doped ZnO nanorods.

The angular dependences of ultrasonic wave velocity (V_L, V_{S1}, V_{S2} and V_D) at different doping percentage are presented in **Figs. 1-4**. The angles are measured form the z-axis of the crystal. Form Fig. 1-2, the velocities V_L and V_{S1} of Gd-doped ZnO nanorods have minima and maxima at 45° respectively with the z-axis of the crystal. Form **Fig. 3**, it finds that V_{S2} increases with angle and have maximum at 55^0 angles. The anomalous behavior of angle dependent velocity is due to combined effect of SOECs and density. The property of the angle dependent velocity curves in this work is similar to nature of angle dependent velocity curve found for other hexagonal type's material [**34,35**]. Thus, the angle dependence of the velocities in nanostructured Gd-doped ZnO nanorods is justified.

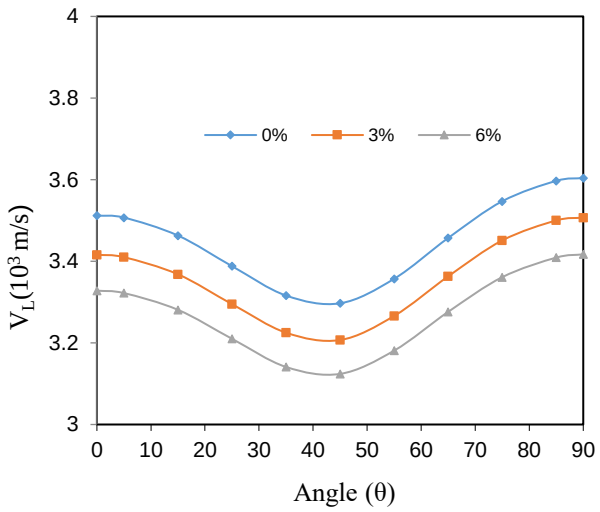

Fig.1. V_L vs angle with z- axis of crystal of % Gd doped ZnO nanorods.

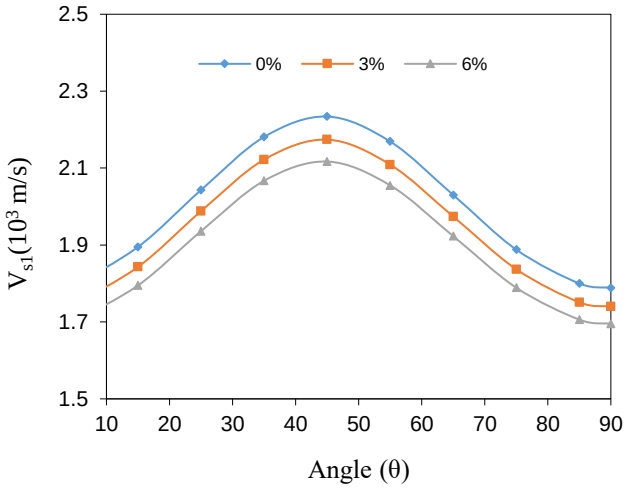

Fig. 2. V_{S1} vs angle with z- axis of crystal of % Gd doped ZnO nanorods.

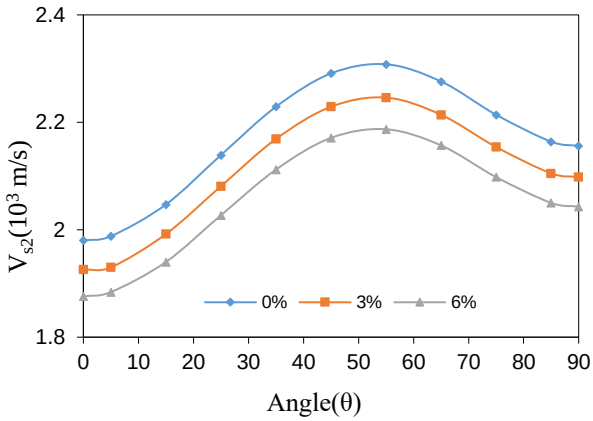

Fig. 3. V_{S2} vs angle with z- axis of crystal of % Gd doped ZnO nanorods.

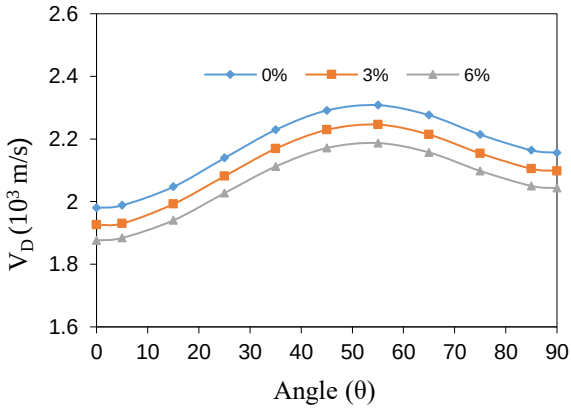

Fig.4. V_D vs angle with z- axis of crystal of % Gd doped ZnO nanorods.

Fig. 4 shows the variation of Debye average velocity (V_D) with the angle made with the z- axis of the crystal. It is clear that V_D increases with the angle and reaches maximum at 55^0 for Gd-doped ZnO nanorods. As the calculation of V_D involves the velocities V_L, V_{S1} and V_{S2} [**36,37**] It is understandable that the variation of debye average velocity is affected by the fundamental ultrasonic velocities. Maximum value of V_D at 55° is due to a

significant decrease in longitudinal wave velocities and an increase in shear wave velocities. It may be determined that the average sound wave velocity is a maximum when a sound wave travels at 55^0 angles with the z- axis of these crystal.

When an ultrasonic wave passes through the medium, it disturbs the equilibrium phonons. These phonons return to their equilibrium state after a certain time called thermal relaxation time 'τ' [**38**]. The variation of thermal relaxation time along different orientations is shown in **Fig. 5**. From the figure, it is clear that thermal relaxation time with doping exhibits opposite trends when compared to the ultrasonic velocities. With increasing concentration of doping, thermal relaxation time increases which is due to the combined effect of the average Debye velocity, thermal conductivity, and specific heat. The minimum value of 'τ' for wave propagation along $\theta = 55^0$ denotes that the re-establishment time for equilibrium distribution of thermal phonons will be minimum for the propagation of wave along this direction. The calculated value of 'τ' is of the order of 10^{-12} s. This shows that the distribution of thermal phonons restores its equilibrium in this time period after passing the sound wave. The information of thermal relaxation time and that of ultrasonic velocity will play a crucial role in the determination of ultrasonic absorption in the medium.

Since $A \propto V^{-3}$ and velocity is the largest for 6% Gd doped ZnO nanorods among 0%Gd, thus the attenuation A should be smallest and material should be most ductile for 6% Gd doped ZnO nanorods.

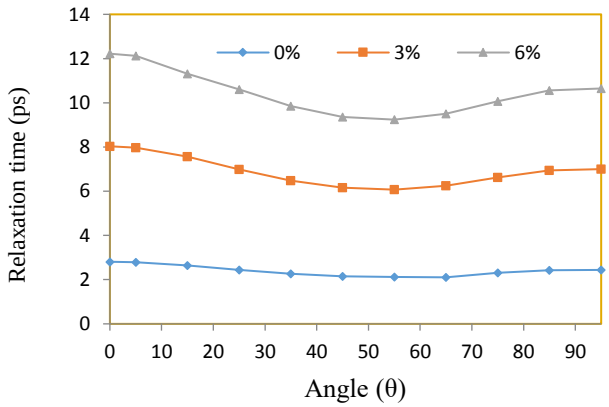

Fig. 5. Relaxation time vs angle with z- axis of crystal of % Gd doped ZnO nanorods.

Conclusion

Based on the above conversation is valuable to state that:

- The principle established on simple interaction potential model remains valid for calculating higher-order elastic coefficients for hexagonally Gd-doped ZnO nanorods.
- Elastic properties of Gd-doped ZnO nanorods imply that this is mechanically stable.
- For Gd-doped ZnO nanorods the thermal relaxation time is found to be of the order of picoseconds, which defends their hexagonal structure. As 'τ' has smallest value along $\theta = 45^0$ for all samples, the time for re-establishment of equilibrium distribution of phonons, will be minimum, for the wave propagation in this direction.
- The mechanical properties of the 6% Gd-doped ZnO nanorods are better than others doped graphene materials.
- Gd-doped ZnO nanorods behave as its purest form for 6% doped graphene and are more ductile demonstrated by the minimum attenuation while at 0% Gd-doped ZnO nanorods are least ductile.

These results will provide a ground for investigating the major thermo physical properties in the field of Gd-doped ZnO nanorods. Nanorods present several advantages, like a larger surface-area to-volume ratio, a direct carrier conduction path, a large variety of potential novel properties available through the control of size and structure, thermal stability and high compatibility with standard industrial device fabrication technologies. Such structures are of particular interest to the researchers; Further intensive research on designed syntheses and easy nanofabrication of nanorods for the large-scale device applications would provide an enormous impact on nanotechnology and open an unprecedented avenue in energy, magnetic, mechanical, electronic, and spintronic applications. However, the future nano technology for nanorods will be dependent on how we can minimize the production cost by maintaining high efficiency and long stability of the devices. Also, study can be beneficial for the processing and non-destructive characterization of nanostructured Gd-doped ZnO nanorods.

Acknowledgment

One of authors (Sachin Rai) is thankful to Council for Scientific and Industrial Research - University Grant Commission (CSIR - UGC) for providing financial assistance in form of CSIR - Junior Research Fellowship (1500/CSIR-UGC NET dec, 2017) India.

Keywords

Gd-doped Nanorods, Elastic properties, Ultrasonic velocity, Thermal relaxation time

References

1. Kumar, R.V.; Diamant, Y.; Gedanken, A.; Sonochemical Chem. Mater., **2000**, *12*, 2305.
2. Liu, Y.; Liao, L.; Li, J.; Pan, C.; J. Phys. Chem. C., **2007**, *111*, 5056.
3. Diao, F.; Wang, Y.; J. Mater Sci., **2018**, *53*, 4334.
4. Nunes, D.; Pimental, A.; Goncalves, A.; Pereira, S.; Branquinho, R.; Barquinha, P.; Furtunato, E.; Martins, R.; Semicond. Sci. Technol., **2019**, *34*, 043001.
5. Sohila, S.; Rajendran, R.; Yaakob, Z.; Teridi, M. A.; Sopian, K.; J. Mater. Sci. Mater. Electron., **2015**, *11*, 4100.
6. Akhavan, O.; Ghaderi, E.; J. Phys. Chem. C., **2009**, *113*, 20214.
7. Yang, Y.; Ren, L.; Zhang, C.; Huang, S.; and Liu, T.; ACS Appl. Mater. Interfaces., **2011**, *3*, 2779.
8. Wang, J.; Tsuzuki, T.; Tang, B.; Hou, X.; Sun, L.; Wang, X.; ACS Appl. Mater. Interfaces., **2012**, *4*, 3084.

9. Fan, H.; Zhao, X.; Yang, J.; Shan, X.; Yang, L.; Zhang, Y.; Li, X.; and Gao, M.; Catal. Commun., **2012**, *29*, 29.
10. Li, B.; Liu, T.; Wang, Y.; and Wang, Z.; J. Colloid Interface Sci., **2012**, *377*, 114.
11. Yin, P. T.; Shah, S.; Chhowalla, M.; and Lee, K. B.; Chem. Rev., **2015**, *115*, 2483.
12. R. Alfonso, J. Xiaoting, H. John, H.; Daniel, N.; Hyungbin, S.; Vladimir, B.; Mildred, S. D.; and Jing, K.; Nano Lett., **2009**, *9*, 35.
13. Liu, N.; Luo, F.; Wu, H.; Liu, Y.; Zhang, C.; and Chen, J.; Adv. Funct. Mater., **2008**, *18*, 1518.
14. Navaneethan, K.; Harish, M.; Ponnusamy, S.; Muthamizhchelvan, C.; Applied Surface Science, **2019**, *34(4)*, 144058.
15. Nikitin, A.; Khramtsov, M.; Garanina, A.; Mogilnikov, P.; Sviridenkova, N.; Shchetinin, I.; Savchenko, A.; Abakumov, M.; Majouga, A.; Journal of Magnetism and Magnetic Materials, **2019**, *469*, 443.
16. Azeem, A.; Ashraf, M.; Munir, U.; Sarwar, Z.; Abid, S.; Iqbal, N.; Journal of Nanotechnology, **2016**, *2016*, 1.
17. Kim, N. W.; Maeng, H. J.; Lee,D. K.; Yu, H.; Journal of Nanoscience and Nanotechnology, **2014**, *14(11)*, 8834.
18. Papageorgiou, D. G.; Kinloch, I. A.; Young, R. J.; Progress in Materials Science, **2017**, *90*, 75.
19. Okpala, C. C.; International Journal of Engineering Research and Development, **2013**, *8(11)*, 17.
20. Yadawa, P. K.; Pramana - J. Phys., **2011**, *76*, 619.
21. Pandey, D. K. Yadawa, P. K.; Yadav, R. R.; Lett., **2007**, *61*, 5198.
22. Voigt, W.; B.G. Teubner., **1966**, 979.
23. Reuss, A.; ZAMM – Journal of Applied Mathematics and Mechanics/Zeitschrift für Angewandte Mathematik und Mechanik., **1929**, *9(1)*, 58.
24. Hill, R.; Proc. Phys. Soc. A., **1952**, *65*, 354.
25. Turkdal, N.; Deligoz, E.; Ozisik, H.; Ozisik, H. B.; Ph. Transit., **2017**, *90*, 609.
26. Weck, P. F.; Kim, E.; Tikare, V.; Mitchell, J. A.; Dalton Tran., **2015**, *44*, 18779.
27. Singh, D.; Pandey, D. K.; Yadawa, P. K.; Yadav, A. K.; Cryogenics., **2009**, *49*, 16.
28. Singh, S. P.; Yadawa, P. K.; Dhawan, P. K.; Verma, A. K.; Yadav, R. R.; Cryogenics., **2019**, *100*, 108.
29. Singh, D.; Yadawa, P. K.; Sahu, S. K.; Cryogenics., **2010**, 50, 479.
30. Yadawa, P. K.; Adv. Mat. Lett., **2011**, *2*, 168.
31. Mohammed, M. O.; Hamad, R. J.; Kutaiba, A.M.; Imad, A. A. H.; Shaker, J. E.; RSC Adv., **2019**, *9*, 33207.
32. Carlotti, G.; Fioretto, D.; Socino, G.; Verona, E.; J. Phys: Condens Matter., 1995, *7*, 9147.
33. Bornstein, L.; American Journal of Physics., **1967**, *35*, 291.
34. Yadav, N.; Singh, S. P.; Maddheshiya, A. K.; Yadawa, P. K.; Yadav, R. R.; Phase Transitions., **2020**, *93*, 894.
35. Yadawa, P. K.; IOP Conf. Series: Materials Science and Engineering., **2012**, *42*, 012034.
36. Yadawa, P. K.; Ceramics-Silikaty., **2011**, *55*, 133.
37. Singh, S. P.; Singh, G.; Verma, A. K.; Yadawa, P. K.; Yadav, R. R.; Pramana - J. Phys., **2019**, *93*, 83.
38. Yadawa, P. K.; Ceramics-Silikaty., **2011**, *55*,133.

Authors biography

Mr. Navin Chaurasiya is an Assistant Professor in the Department of Mechanical Engineering, Veer Bahadur Singh Purvanchal University. He is pursuing Ph.D. in Prof. Rajendra Singh (Rajju Bhaiya) Institute of Physical Sciences for Study and Research, Veer Bahadur Singh Purvanchal University, Jaunpur, Uttar Pradesh, India. His current interests of research include the synthesis of metal oxides nanoparticles, nanocomposite materials, etc.,

Mr. Sachin Rai is pursuing Ph.D. in Prof. Rajendra Singh (Rajju Bhaiya) Institute of Physical sciences for Study and Research, V. B. S. Purvanchal university, Jaunpur (U.P), India. His area of research includes the "Synthesis of non-destructive characterization nanomaterials". Currently, He is **Senior Research Fellow SRF**, sponsored by UGC, New Delhi.

Dr. Pramod Kumar Yadawa is an Associate Professor in the Department of Physics and Founder Director of Prof. Rajendra Singh (Rajju Bhaiya) Institute of Physical sciences for Study and Research, V. B. S. Purvanchal university, Jaunpur (U.P), India. He obtained his Ph. D. degree in Ultrasonic from University of Allahabad, Pryagraj, India. His research interest is the ultrasonic non-destructive testing (NDT) characterization of condensed materials, nanofluids etc. He is the life member of USI, IAPT, MRSI. He is member of International Association of Engineers. He has been awarded by Best Teacher Award 2016 by ASET, New Delhi. He has published 53 research papers in peer reviewed journals.

Graphical abstract

The elastic, mechanical and thermal properties of Gd-doped ZnO nanorods (NRs) have been studied using Lenard Jones potential interaction potential model. The orientation dependent ultrasonic velocities and thermal relaxation time have been evaluated for the determination of anisotropic behaviour and thermophysical properties. The mechanical properties of the Gd-doped ZnO nanorods are better than at 6% Gd amount due to minimum attenuation.

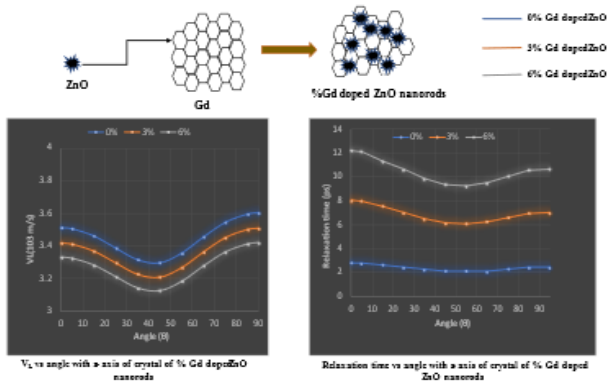

V_L vs angle with a axis of crystal of % Gd dopedZnO nanorods

Relaxation time vs angle with a axis of crystal of % Gd doped ZnO nanorods